

Observation of hypertritons in Au+Au collisions at $\sqrt{s_{\text{NN}}} = 200 \text{ GeV}$

J H Chen^{1,2} for the STAR Collaboration

¹*Physics department, Kent State University, Kent, OH, 44242, USA*

²*Division of nuclear physics, Shanghai Institute of Applied Physics, CAS, Shanghai, 201800, China*

Abstract

We report preliminary results of ${}^3_{\Lambda}\text{H}$ observation in heavy-ion collisions at RHIC. We have identified 157 ± 30 candidates in the current sample containing $\sim 10^8$ Au+Au events at $\sqrt{s_{\text{NN}}} = 200 \text{ GeV}$. The production rate of ${}^3_{\Lambda}\text{H}$ is close to that of ${}^3\text{He}$. No extra penalty factor is observed for ${}^3_{\Lambda}\text{H}$, in contrast to results observed at the AGS.

1. Introduction

Hypernuclear physics opens a unique opportunity for the study of the hyperon-nucleon (YN) and the hyperon-hyperon (YY) interaction. A hypernucleus has a non-zero strangeness quantum number, and thus for nuclear spectroscopy, it provides one more degree of freedom than a normal nucleus containing only protons and neutrons. Information on the strangeness sector of the hadronic equation of state is crucial for understanding the structure of a neutron star. Depending on the strength of the YN interaction, a neutron star might be a hyperon star, or strange quark matter, or might have a kaon condensate at its core [1]. The lightest and simplest hypernucleus is the hypertriton (${}^3_{\Lambda}\text{H}$), consisting of a Lambda, a proton and a neutron. The hypernucleus was first observed in 1952 [2], while no anti-hypernucleus has been found yet.

The Relativistic Heavy-Ion Collider produces a system that consists of a large number of particles with high phase-space density, and with almost equal numbers of quarks and anti-quarks. This environment is uniquely suited for production of exotic nuclei, including hypernuclei, anti-nuclei, and anti-hypernuclei.

2. Analysis and Results

In this paper, we report STAR preliminary results on ${}^3_{\Lambda}\text{H}$ measurement in Au+Au collisions at $\sqrt{s_{\text{NN}}} = 200 \text{ GeV}$. The signal candidates were reconstructed in the central TPC [3] and were identified via the secondary vertex of ${}^3_{\Lambda}\text{H} \rightarrow {}^3\text{He} + \pi^-$. Approximately 2.3×10^7 minimum-bias (MB) trigger events and 2.2×10^7 central trigger events from Au + Au data collected in the year 2004 run, and 6.8×10^7 MB events in the year 2007 Au+Au run have been used in this analysis. Events were required to have a primary vertex position within 30 cm from the center

Email address: jhchen@rcf.rhic.bnl.gov (J H Chen^{1,2} for the STAR Collaboration)

Preprint submitted to Nuclear Physics A

August 14, 2019

of the TPC along the beam direction. Charged tracks were reconstructed in the STAR TPC for pseudorapidity $|\eta| < 1.8$ with full azimuthal acceptance ($0 \leq \phi \leq 2\pi$).

Particle identification is achieved by correlating the ionization energy loss (dE/dx) of charged particles in the TPC gas with their measured magnetic rigidity (Fig 1, left panel). Since the $\langle dE/dx \rangle$ distribution for a fixed particle type is not Gaussian, a new variable z_i ($i = \pi, K, p, d, t, {}^3\text{He}, \dots$) is useful in order to facilitate deconvolution into Gaussians for each particle species [4]. The z_i is defined as $z_i = \ln(\langle dE/dx \rangle / \langle dE/dx \rangle_i^B)$, where $\langle dE/dx \rangle_i^B$ is the expected value of $\langle dE/dx \rangle$ for the given particle type [5]. We are only able to identify ${}^3\text{He}$ with larger momenta (i.e., $p > 2 \text{ GeV}/c$). Furthermore, the beam pipe causes contamination of the ${}^3\text{He}$ sample. Since most beam pipe knock-out ${}^3\text{He}$ are far away from the collision vertex, a cut on distance of closest approach to the collision vertex (DCA $< 1 \text{ cm}$) reduces the background associated with the beam pipe. Fig 1 (right panel) shows the ${}^3\text{He}$ candidate distributions before and after the DCA cut. The condition $|z_{{}^3\text{He}}| < 0.2$ with the 1-cm DCA cut are used in this analysis. The daughter pion from the ${}^3\Lambda^0$ H decay usually has a relatively low momentum, and it can be cleanly identified with similar $\langle dE/dx \rangle$ selection in our experiment (Fig 1, left panel) [4].

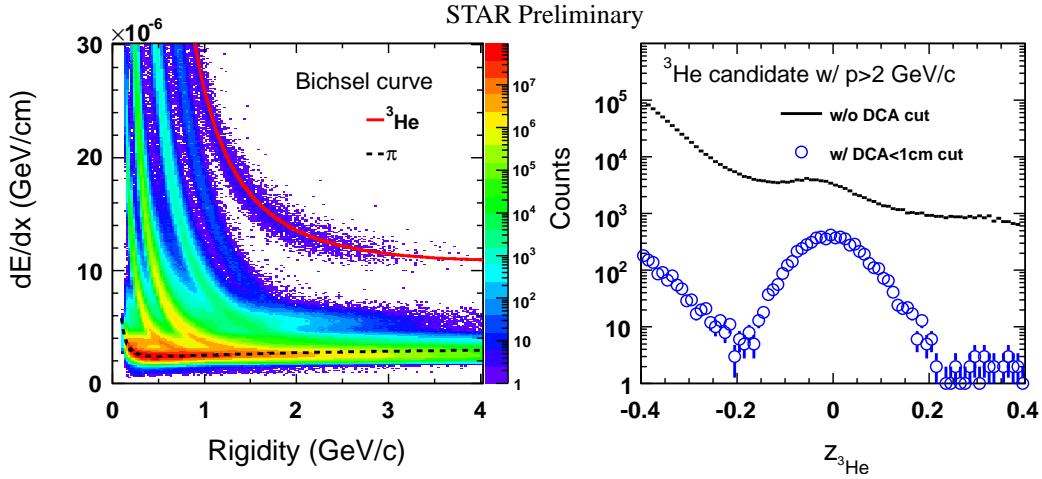


Figure 1: The left panel shows dE/dx versus rigidity for charge particles reconstructed in the STAR TPC. Different bands represent different particle types. The expected curves for ${}^3\text{He}$ and π are also plotted. The right panel shows the $z_{{}^3\text{He}}$ distribution for ${}^3\text{He}$ candidates at $p > 2 \text{ GeV}/c$. The black line represents the data without a DCA cut, and the open circles show the result with DCA $< 1 \text{ cm}$.

With both daughter candidates identified, we can reconstruct the signal through its weak decay topology. A set of topological cuts has been applied here in order to reduce the combinatorial background. The cuts include: DCA between ${}^3\text{He}$ and pion tracks ($< 1 \text{ cm}$), DCA of the ${}^3\Lambda^0$ H candidate to the primary vertex ($< 1 \text{ cm}$), decay length of the ${}^3\Lambda^0$ H candidate vertex from the collision vertex ($> 2.4 \text{ cm}$), and the DCA of the pion daughter to the primary vertex ($> 0.8 \text{ cm}$). The cuts were optimized based on a full detector response simulation [4]. The secondary vertex finding technique used in our experiment is essential for this rare particle search because it can reduce the background dramatically.

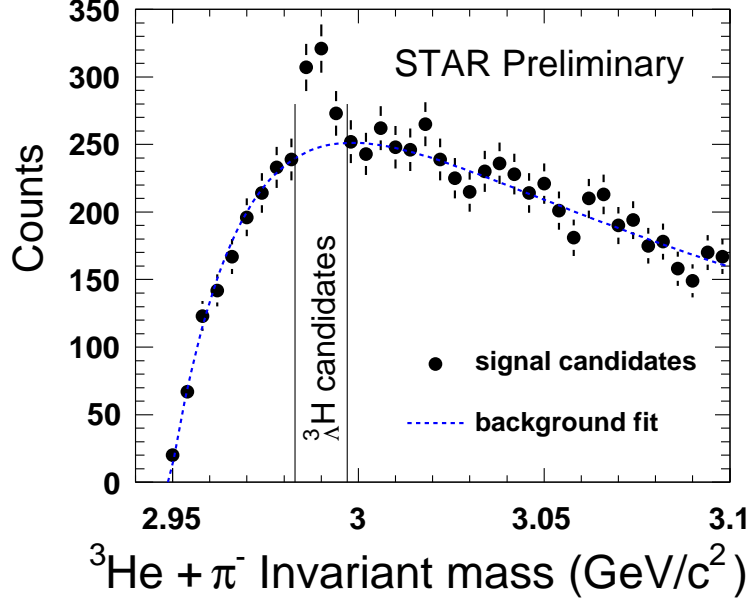


Figure 2: STAR preliminary invariant mass distribution for the daughters ${}^3\text{He} + \pi^-$ in Au+Au collisions at $\sqrt{s_{\text{NN}}} = 200$ GeV. The solid circles represent the signal candidate distribution, and the dashed line is the corresponding fitted background distribution.

Fig. 2 shows the invariant mass distribution of ${}^3\text{He} + \pi^-$ with all cuts applied. The solid circles represent the signal candidate distribution while the dashed curve is the corresponding background distribution. The signal candidate invariant mass was calculated based on the momenta of the daughter candidates at the decay vertex: $M^2 = E^2 - P^2$, $E = E_{{}^3\text{He}} + E_\pi$, $\vec{P} = \vec{P}_{{}^3\text{He}} + \vec{P}_\pi$. The background distribution is produced by the event rotation method. Instead of directly subtracting the background from the data, we use a fitting function. Here we use a double exponential function: $f(x) \propto \exp(-\frac{x}{p_1}) - \exp(-\frac{x}{p_2})$ to fit the background distribution, where p_1, p_2 are fitting parameters. The signal is then counted after subtraction of the fitted rotated background. In total, 157 ± 30 ${}^3_\Lambda\text{H}$ candidates were found in the current data sample. A very similar analysis can be used to search for anti-hypertritons decaying to ${}^3\bar{\text{He}} + \pi^+$. Results of this search are reported elsewhere.

Fig. 3 shows the preliminary ${}^3_\Lambda\text{H}$ p_t spectra together with the ${}^3\text{He}$ results in the same data set. The results are corrected for detector acceptance and tracking efficiency. Since we combine the MB and central trigger data for this analysis, we here normalize the invariant yield per event per participant pair: $(N_{\text{eve}}^{\text{MB}} \times N_{\text{part}}^{\text{MB}} + N_{\text{eve}}^{\text{central}} \times N_{\text{part}}^{\text{central}})/2$ rather than the conventional number of total events: N_{eve} . We then compare the ${}^3_\Lambda\text{H}$ production rate with ${}^3\text{He}$ in our data. It is quite surprising to observe that their production ratio is close to unity. This is different from the value obtained at the AGS, where an extra penalty factor has been observed when introducing the strangeness degree of freedom in particle production [6]. It seems that our results cannot be solely due to the finite size effect as implied by AGS data [6]. In contrast, our measurements indicate that at

RHIC, the strangeness phase space population is similar to that of light quarks.

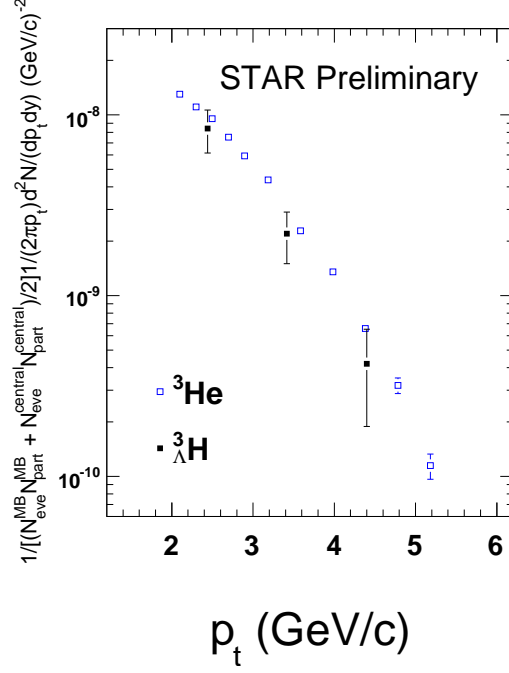


Figure 3: STAR preliminary results on ${}^3\text{H}$ and ${}^3\text{He}$ invariant yield vs. p_t . The results have been corrected for detector acceptance and tracking efficiency. The error bars represent statistical uncertainties only.

3. Summary

In summary, we present preliminary ${}^3\text{H}$ measurements in Au+Au collisions at $\sqrt{s_{\text{NN}}} = 200$ GeV. We have collected 157 ± 30 signal candidates in the current statistics. Our measurement of the ${}^3\text{H}/{}^3\text{He}$ ratio is consistent with the enhancement of strangeness production at RHIC.

References

- [1] J. M. Lattimer, M. Prakash, Science 304 (2004) 536.
- [2] M. Danysz, J. Pniewski, Phil. Mag. 44 (1953) 348.
- [3] M. Anderson, et al., Nucl. Instrum. Methods A 499 (2003) 659.
- [4] B. I. Abelev, et al., Phys. Rev. C 79 (2009) 034909.
- [5] C. Amsler, et al., Phys. Lett. B667 (2008) 1.
- [6] T. A. Armstrong, et al., Phys. Rev. C 70 (2004) 024902.